6. Cooke CD, Garcia EV, Cullom SJ, Faber TL, Pettigrew RI. Determining the accuracy of calculating systolic wall thickening using a fast Fourier transform approximation: a simulation study based on canine and patient data. *J Nucl Med* 1994;35:1185–1192.
7. Germano G, Kiat H, Kavanaugh PB, et al. Automatic quantification of ejection fraction from gated myocardial perfusion SPECT. *J Nucl Med* 1995;36:2138–2147.
8. Nichols K, DePuey EG, Salensky H, Rozanski A. Reproducibility of ejection fractions from stress versus rest gated perfusion SPECT [Abstract]. *J Nucl Med* 1996;37:115P.
9. Nichols K, DePuey EG, Rozanski A. Automation of gated tomographic left ventricular ejection fraction. *J Nucl Cardiol* 1996;3:475–482.
10. Everaert H, Franken PR, Flamen P, Momen A, Bossuyt A, Goris ML. Radial distribution of myocardial count rate density to measure left ventricular ejection fraction from gated perfusion SPECT studies [Abstract]. *J Nucl Med* 1996;37:211P.
11. Williams KA, Taillon LA. Left ventricular function in patients with coronary artery disease assessed by gated tomographic myocardial perfusion images: comparison with assessment by contrast ventriculography and first-pass radionuclide angiography. *J Am Coll Cardiol* 1996;27:173–181.
12. Vansant JP, Faber TL, Folks RD, Rao JM, Garcia EV. Resting left ventricular volumes and ejection fraction from gated SPECT: correlation to first pass [Abstract]. *Circulation* 1996;92(suppl I):I-11.
13. Lefkowitz D, Nichols K, Rozanski A, Horowitz R, Mogtader A, DePuey EG. Echocardiographic validation of left ventricular volume measurements by ^{99m}Tc-sestamibi gated SPECT [Abstract]. *J Am Coll Cardiol* 1996;27:241A.
14. Faber TL, Stokely EM, Peshock RM, Corbett JR. A model-based four-dimensional left ventricular surface detector. *IEEE Trans Med Imaging* 1991;10:321–329.
15. Mullick R, Ezquerra NF. Automatic determination of LV orientation from SPECT data. *IEEE Trans Med Imaging* 1995;14:88–99.
16. Germano G, Kavanaugh PB, Chen J, et al. Operator-less processing of myocardial perfusion SPECT studies. *J Nucl Med* 1995;36:2127–2132.
17. DePuey EG. Artifacts in SPECT myocardial perfusion imaging. In: DePuey EG, Berman DS, Garcia EV, eds. *Cardiac SPECT*. New York: Raven Press; 1995:169–200.
18. DePuey EG, Rozanski A. Using gated technetium-99m-sestamibi SPECT to characterize fixed myocardial defects as infarct or artifact. *J Nucl Med* 1995;36:952–955.
19. Williams KA, Taillon LA. Reversible ischemia in severe stress technetium-99m-labeled sestamibi perfusion defects assessed from gated single-photon emission computed tomographic polar map Fourier analysis. *J Nucl Cardiol* 1995;2:199–206.
20. Van Train KF, Areeda J, Garcia EV, et al. Quantitative same-day rest-stress

technetium-99m-sestamibi SPECT: definition and validation of stress normal limits and criteria for abnormality. *J Nucl Med* 1993;34:1494–1502.
21. DePuey EG, Nichols KJ, Slowikowski JS, et al. Fast stress and rest acquisitions for technetium-99m-sestamibi separate-day SPECT. *J Nucl Med* 1995;36:569–574.
22. Nichols K, DePuey EG, Gooneratne N, Salensky H, Friedman M, Cochoff S. First-pass ventricular ejection fraction using a single crystal nuclear camera. *J Nucl Med* 1994;35:1292–1300.
23. Crawford CR. CT filtration aliasing artifacts. *IEEE Trans Med Imaging* 1991;10:99–102.
24. Hoffman EJ, Huang SC, Phelps ME. Quantitation in positron emission computed tomography. I. Effects of object size. *J Comput Assist Tomogr* 1979;5:391–400.
25. Gradel C, Staib LH, Heller EN, et al. Limitations of ECG-gated SPECT for assessment of regional thickening: experimental comparison with ECG-gated MRI [Abstract]. *J Am Coll Cardiol* 1996;27:241A.
26. Bland JM, Altman DG. Statistical methods for assessing agreement between two methods of clinical measurement. *Lancet* 1986;1:307–310.
27. Bland JM, Altman DG. A note on the use of the interclass correlation coefficient in the evaluation of agreement between two methods of measurement. *Comput Biol Med* 1990;20:337–340.
28. Johnson LL, Verdesca SA, Xavier RC, Chang KK, Nott LT, Noto RB. Postischemic stunning affects wall motion scores on poststress gated sestamibi tomograms [Abstract]. *J Am Coll Cardiol* 1996;27(suppl):241A.
29. Williams KA, Taillon LA. Five methods for evaluation of left ventricular function with ^{99m}Tc-sestamibi: a comparison with contrast ventriculography [Abstract]. *J Nucl Med* 1996;37:104P.
30. Williams KA, Lang RM, Reba RC, Taillon LA. Comparison of technetium-99m-sestamibi gated tomographic perfusion imaging with echocardiography and electrocardiography for determination of left ventricular mass. *Am J Cardiol* 1996;77:750–755.
31. Galt JR, Garcia EV, Robbins WL. Effects of myocardial wall thickness of SPECT quantification. *IEEE Trans Med Imaging* 1990;9:144–150.
32. Faber TL, Cooke CD, Vansant JP, Garcia EV. Sensitivity of an automated ejection fraction calculation from gated perfusion tomograms to modeling assumptions [Abstract]. *J Nucl Med* 1996;37:213P.
33. Buvat I, Bacharach SL, Bartlett ML, Yaroslavsky L. Wall thickening from gated SPECT/PET: evaluation of four methods [Abstract]. *J Nucl Med* 1995;36:8P.

Relationship of Decreased Chemotaxis of Technetium-99m-HMPAO-Labeled Lymphocytes to Apoptosis

C. Van de Wiele, J. Philippé, J.P. Van Haelst, J. Van Damme, H. Thierens, G.E. Leroux-Roels and R.A. Dierckx

Division of Nuclear Medicine; Department of Clinical Chemistry, Clinical Microbiology and Immunology; and Department of Medical Physics, University Hospital Gent, Gent; REGA Institute, Laboratory of Molecular Immunology, University Leuven, Leuven, Belgium

The purpose of this study was to evaluate chemotaxis and its relationship to apoptosis in ^{99m}Tc-HMPAO-labeled lymphocytes. **Methods:** Peripheral lymphocytes, obtained from 12 healthy volunteers using lymphoprep, were divided in three equal fractions. One fraction was used as the control, one was labeled with cold HMPAO and one was labeled with 1.5 mCi (55.5 Mbq) ^{99m}Tc-HMPAO. Chemotaxis of T-lymphocytes was measured by the Boyden microchamber technique (BMA) (n = 8) using human monocyte chemotactic protein-3 (MCP-3) as chemoattractans. A chemotactic index was calculated as the number of HMPAO and ^{99m}Tc-HMPAO-labeled cells that migrated towards the MCP-3 solution, divided by the number of nonlabeled migrated lymphocytes. Apoptosis evaluation (n = 10) of unlabeled, HMPAO-labeled and ^{99m}Tc-HMPAO-labeled cells was performed using flowcytometry (FCM) forward light scatter analysis, 90O light scatter analysis, fluorescein-isothiocyanate (FITC)-labeled Annexin V and dye exclusion of propidium iodide. **Results:** Chemotaxis of ^{99m}Tc-HMPAO-labeled T-lymphocytes was found to be reduced by approximately 31% (migration index of 0.69) (p = 0.01) as compared to both unlabeled and HMPAO-labeled lymphocytes, both the latter showing no difference in migration index. Whereas the mean percentages apoptotic lym-

phocytes in the unlabeled, 18.5%, and HMPAO-labeled fraction, 16.6%, were more or less comparable (p = 0.1), the mean percentage apoptotic cells in the ^{99m}Tc-HMPAO-labeled fraction was 51.8%, yielding a difference of 33.3% between ^{99m}Tc-HMPAO-labeled and unlabeled cells (p = 0.003). The procentual concordance between apoptotic cells (33.3%) and chemotactic impaired cells (31%) in the ^{99m}Tc-HMPAO-labeled fraction may be explained by the formation of a rigid cytoskeleton early in the apoptotic process that may theoretically limit chemotaxis. **Conclusion:** Using the BMA, chemotaxis of ^{99m}Tc-HMPAO-labeled lymphocytes was found to be reduced by approximately 31%. Furthermore, the percentage apototic lymphocytes induced by irradiation after labeling with ^{99m}Tc-HMPAO concurs well with the percentage of chemotaxis impaired cells.

Key Words: technetium-99m-HMPAO-labeled lymphocytes; apoptosis; chemotaxis

J Nucl Med 1997; 38:1417–1421

Controversy has surrounded the diagnostic value of labeling pure granulocytes as opposed to a mixed leukocyte population. In a study by Schauwecker et al. (*1*), comparing mixed leukocytes and pure granulocytes labeled in plasma, mixed leukocytes showed a slightly greater sensitivity for detecting

chronic infections. This was hypothetically attributed to the presence of labeled lymphocytes in the reinjected mixed-cell suspension and a predominantly lymphocytic response in the chronic stage of infection. However, whereas chemotaxis of ^{99m}Tc-HMPAO-labeled granulocytes has been thoroughly examined (2,3), no exact data on chemotaxis of ^{99m}Tc-HMPAO-labeled lymphocytes are available (4). After irradiation, lymphocytes undergo apoptosis, a process which in an early stage is characterized by condensation of cytoplasm through the formation of a rigid cytoskeleton which may theoretically limit chemotaxis (5).

The term apoptosis was coined to describe a type of cell death, different from necrosis. Necrosis is associated with irregular clumping of chromatin, marked swelling of organelles and focal disruption of membranes that subsequently disintegrate, until removed by mononuclear phagocytes. On the other hand, apoptosis is characterized by compaction and margination of nuclear chromatin, condensation of cytoplasm and convolution of nuclear and cellular outlines in an early stage (6). At a later stage, the nuclear fragments and protuberances that form on the cell surface separate to produce apoptotic bodies that are phagocytosed by nearby cells and degraded by lysosomal enzymes (7,8).

The classic methods of detecting apoptosis include microscopy and internucleosomal DNA fragmentation determination. However, the widespread use of in vitro cell systems for studying cell death has led many researchers to turn to flow cytometry as an alternative to these classic methods. Flow cytometry offers many advantages over the aforamentionned methods due to its capability to analyze individual cells, the ease of cell sample preparation, rapidity of sample analysis and low cell number required (9). Hence, the aim of this study was to evaluate chemotaxis and its relation to apoptosis in ^{99m}Tc-HMPAO-labeled lymphocytes as determined by flow cytometry.

MATERIALS AND METHODS

Isolation and Preparation of Lymphocytes

Forty milliliters venous blood were repeatedly collected from 12 healthy donors in sterile disposable tubes, containing preservative-free heparin. There were six women and six men, mean age 44 yr, age range 23–62 yr. After dilution in 0.9% (w/v) NaCl in a 1/1 ratio, the diluted blood suspension of 80 ml was placed on 60 ml lymphoprep (Nycomed, Brussels, Belgium), a mixture of sodium metrizoate and Ficoll. After centrifugation at 200 g during 20 min, the interface layer containing lymphocytes, monocytes and platelets was collected and washed with 10 ml Hanks balanced salt solution (HBSS) containing 0.5% human serum albumin (HSA) to reduce the number of contaminating platelets. The lymphocyte pellet, obtained after centrifugation at 150 g for 10 min, was resuspended in 1.7 ml HBSS + 0.5% HSA. Of this suspension, 0.2 ml was diluted in 0.8 ml HBSS + 0.5% HSA and used for cell counting. The remaining 1.5-ml cell suspension was divided in three fractions, A, B and C, of 0.5 ml each. Subsequently, 0.1 ml HBSS + 0.5% HSA was added to Fraction A, 0.1 ml HMPAO solution containing 16.7 μg HMPAO was added to Fraction B and 0.1 ml ^{99m}Tc-HMPAO containing 16.7 μg HMPAO and 1.5 mCi (55.5 MBq) ^{99m}Tc, was added to Fraction C. After incubation for 15 min, all three fractions were centrifuged at 150 g for 5 min. Finally, the pellet of all three fractions was resuspended in HBSS + 0.5% HSA.

Radiolabeling

The HMPAO solution was obtained by injecting 2 ml 0.9% (w/v) NaCl into the vial containing 0.5 mg HMPAO (Ceretec,

Amersham International plc, Green End Aylesbury, United Kingdom). This solution was divided in two equal fractions. Thereafter, 0.1 ml of the first fraction, mixed with 0.5 ml 0.9% (w/v) NaCl, was added to cell Fraction B. The second fraction was gently mixed with 22.5 mCi (832.5 Mbq) ^{99m}Tc, dissolved in 0.5 ml 0.9% (w/v) NaCl. Subsequently, 0.1 ml of this solution containing 1.5 mCi (55.5 Mbq) ^{99m}Tc-HMPAO was added to cell Fraction C and incubated for 15 min. The dose of 1.5 mCi approximates the relative dose usually administered to lymphocytes in a mixed cell population (10). Finally, the labeling efficiency of cell Fraction C was determined as 100 × the count of the washed cell suspension over the total count.

Cell Counting

Cell counting of the samples was performed with the Coulter STKS system (Coulter Electronics Limited, Luton, United Kingdom).

Chemokine

Human monocyte chemotactic protein-3 (MCP-3) synthesized on a model 431 A solid-phase peptide synthesizer (Applied Biosystems, Foster City, CA) using Fmoc protecting groups was used as chemoattractant for lymphocytes (11).

Chemotaxis Assay

Chemotaxis was measured by the Boyden microchamber technique (n = 8) (12). In all eight experiments, the number of contaminating monocytes in the cell suspension was ≤5%. The lower compartment of the microchamber was filled with 27 μl MCP-3 solution, concentration 10 ng/mL, and separated from the upper compartment by a 5-μm pore-size polycarbonate membrane (polyvinylpyrrolidone treated for lymphocytes). The upper wells (n, number of wells filled per cell fraction = 3) were filled with 50-μl cell suspension of Fractions A, B and C, containing approximately 500,000 lymphocytes, in HBSS supplemented with 0.5% HSA and incubated for 240 min at room temperature. After incubation, the membranes were removed from the microchambers and the cells were fixed and stained with Diff-Quick (modified Wright staining). Migrated lymphocytes were counted in 10 microscopic fields per well and the mean count of three wells was used as representative value for each fraction. The chemotactic index was calculated as the number of HMPAO-labeled and ^{99m}Tc-HMPAO-labeled lymphocytes that migrated towards the MCP-3 solution, divided by the number of nonlabeled migrated lymphocytes. The migration index of nonlabeled lymphocytes represents a value of 1.0, whereas the value of labeled lymphocytes, either HMPAO or ^{99m}Tc-HMPAO labeled can give a migration index different from 1.0.

Evaluation of Apoptosis

For apoptosis evaluation (n = 10), Fractions A, B and C were diluted in RPMI 1640 containing 2 μmol L-glutamine, 0.5% HSA and Hepes buffer (Gibco, Paisley, United Kingdom), supplemented with 50N/ml penicillin and 50 μg/ml streptomycine, to a final concentration of 10^6 cells/ml. A sample of 1 ml of each fraction was obtained and incubated at 37°C for 24 hr in a 5% CO_2 atmosphere. After incubation all three samples were analyzed by flowcytometry (FCM). FCM can reveal apoptotic lymphocytes in unstained preparations on the basis of the decrease in forward light scatter signal combined with the increase in 90° light scatter that occurs as a result of cellular shrinkage and increased internal granularity or density (9,13).

This assay is effective with either viable or fixed lymphocytes, making it convenient for routine analysis. Furthermore, using FCM, cell staining for Annexin V was evaluated with fluorescein isothiocyanate (FITC)-labeled Annexin V (Bender Medsystems, Vienna, Austria), combined with dye exclusion of propidium

TABLE 1
Chemotaxis Assay

Experiment	Unlabeled cells	Migration index	
		HMPAO-labeled cells	^{99m}Tc-HMPAO-labeled cells
1	1	1.01	0.67
2	1	1.01	0.63
3	1	0.99	0.67
4	1	1.05	0.66
5	1	0.98	0.71
6	1	0.97	0.70
7	1	0.96	0.73
8	1	0.98	0.71
s.d.		Mean 0.99	Mean 0.69
		0.03	0.03 s.d.

iodide (PI) (Sigma Chemical Co., St. Louis, MO). Annexin V, a Ca^{2+}-dependent phospholipid-binding protein, allows detection of the redistribution of phosphatidylserine (PS), which is normally confined to the inner plasma membrane leaflet but becomes externalized early during apoptosis (14,15). Propidium iodide, a fluorochrome that intercalates in the groove between the two strands of the DNA double helix, allows detection of late apoptotic cells that have become permeable to the dye (16). The combination of light scatter analysis, Annexin V analysis and PI-fluorescence allows differentiation between lymphocytes in early phase apoptosis (low FLS, AnnexinV+ and low PI staining) and lymphocytes in late-phase apoptosis (low FLS, AnnexinV+ and high PI staining) (13). FCM was performed 24 hr following labeling with ^{99m}Tc-HMPAO since practical experience at the Department of Clinical Biology has shown this to be the optimal moment for apoptosis analysis of irradiated lymphocytes. In general, 4 hr following irradiation of lymphocytes, only slight differences in apoptosis between irradiated and nonirradiated lymphocytes are found.

Statistical Analysis

Statistical analysis was performed using the nonparametric Wilcoxson sign test.

TABLE 2
Percentage Apoptotic Cells

Experiment	Unlabeled		HMPAO-labeled		^{99m}Tc-HMPAO-labeled	
	A	A+P	A	A+P	A	A+P
1	3.7	20.3	3.6	23.8	5.3	37.0
2	1.3	23.9	2.8	12.4	21.0	53.2
3	3.0	11.9	2.7	10.4	14.5	49.0
4	5.8	12.3	3.8	15.0	13.1	29.9
5	6.08	16.5	4.7	16.6	11.1	44.4
6	2.1	13.9	1.4	7.7	7.5	27.7
7	4.0	28.1	2.6	24.6	31.0	41.0
8	4.3	13.0	1.7	8.8	5.8	31.5
9	2.8	6.1	1.0	17.7	11.5	39.1
10	1.3	4.4	1.1	4.0	5.4	39.4
Mean	3.4	15.0	2.5	14.1	12.6	39.2
s.d.	1.7	7.4	1.2	6.8	8.1	8.2
Mean (A+P)/ Mean (A)		4.4		5.6		3.1
Mean A+(A+P)		18.5		16.6		51.8
s.d. A+(A+P)		7.8		7.5		14.0

RESULTS

Cell Counting and Labeling Efficiency

The number of mononuclear cells after isolation with lymphoprep varied from 205.6 × 10^6/40 ml to 1126 × 10^6/40 ml (mean 12.03 × 10^6/ml; range 5.14 × 10^6/ml to 28.15 × 10^6/ml). The mean percentage lymphocytes was 80.03% (range: 53.83%–99.71%), the mean percentage monocytes was 10.9% (range: 0,03%–45.84%).

For the chemotaxis assay, only cell suspensions containing ≤5% monocytes were used (mean % monocytes 1.24%; range: 0,03-5%). Labeling efficiency varied from 8.26% to 24% (mean 16.02%). The specific activity per lymphocyte varied from 11 μCi (403 kBq)/10^6 lymphocytes to 93.4 μCi (3.09 MBq)/10^6 lymphocytes (μ = 30 μCi/10^6 lymphocytes, s.d. = 22.7 μCi (840 kBq)/10^6 lymphocytes).

Chemotaxis Assay

Results of the Boyden microwell chamber assay are shown in Table 1. Using the Boyden microwell chamber assay, chemotaxis of ^{99m}Tc-HMPAO-labeled T-lymphocytes, was found to be reduced by approximately 31% (migration index of 0.69) as compared to both nonlabeled and HMPAO-labeled controls (p = 0.01), both the latter showing no difference in migration index (statistical insignificant).

Apoptosis Evaluation

Results of the apoptosis assay are shown in Table 2. The mean percentage apoptotic lymphocytes in the unlabeled (μ = 18.5%; s.d. = 7.8%) and HMPAO-labeled fraction (μ = 16.6%; s.d. = 7.5), was more or less comparable (p = 0.1). The mean percentage apoptotic cells in the ^{99m}Tc-HMPAO-labeled fraction was 51.8% (s.d. = 14.0%), yielding a mean difference of 33.3% between ^{99m}Tc-HMPAO-labeled and unlabeled cells (p = 0.003). In order to allow comparison with the chemotactic assay, fetal calf serum was not added to the HBSS solution used since it contains lymphocyte growth factors in addition to being a nutritious agent for lymphocytes. This may account for the high contribution of late apoptotic cells in all three cell fractions. The contribution of early and late apoptotic cells to the total of apoptotic cells was more or less comparable for both the unlabeled and HMPAO-labeled cell fraction as shown by their comparable ratio of mean percentage of late over early apoptotic cells of 4.4 and 5.6, respectively. In the ^{99m}Tc-HMPAO-labeled fraction, a higher relative number of early apoptotic cells was present as compared to both unlabeled and HMPAO-labeled fractions as shown by its ratio of mean percentage of late over early apoptotic cells of 3.1. Figure 1A and B illustrates the results obtained by flow cytometry for a control sample (unlabeled) and a sample labeled with ^{99m}Tc-HMPAO.

DISCUSSION

In response to infection, white blood cell infiltration into the inflammatory focus is mediated by chemotactic cytokines or chemokines. These chemokines are classified into two subfamilies depending on the arrangement of the first two of four conserved cysteines, which are separated by one amino acid (CXC chemokines) or are adjacent (C-C chemokines) (17,18). Contrary to the classical chemotactic agents, such as formyl-methionyl-leucyl-phenylalanine (FMLP), platelet-activating factor (PAF) and complement factor 5a (C5a), these chemokines selectively attract and activate distinct leukocyte populations. Whereas CXC chemokines act preferentially on neutro-
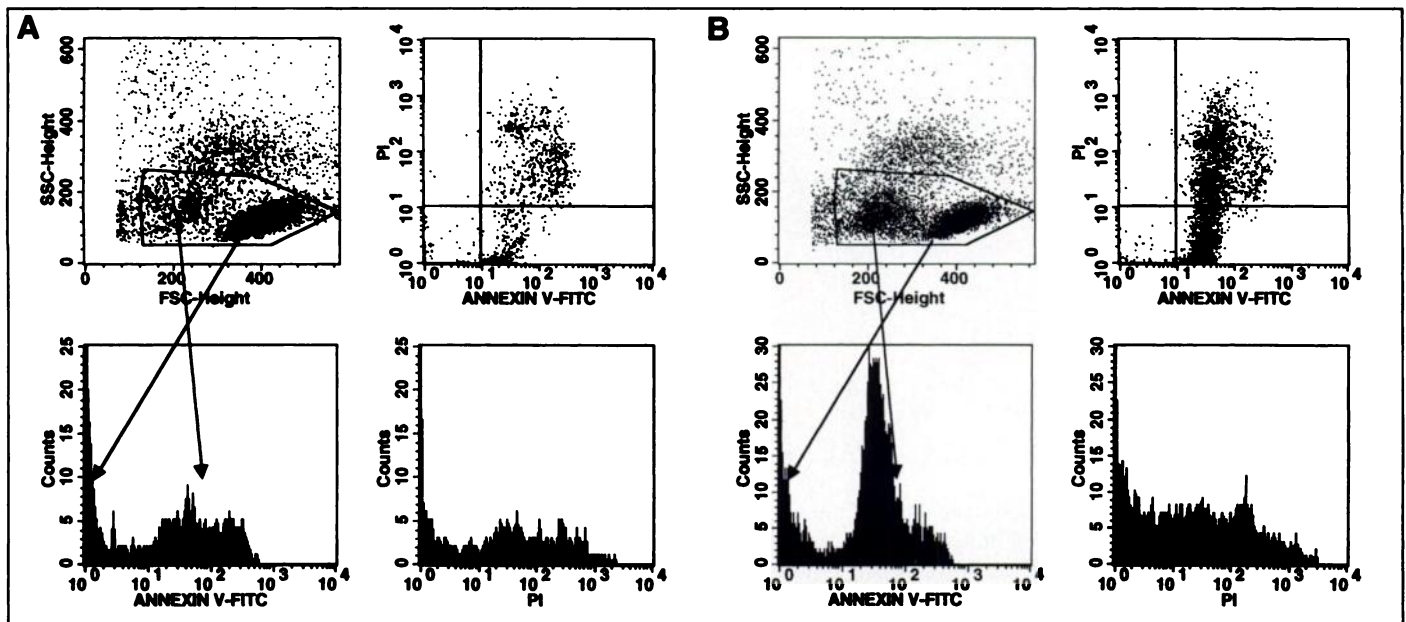
FIGURE 1. (A) The flowcytometric plots of a 24-hr culture of control cells. In the FSC/SSC diagram a gate is drawn around the lymphocytes. In the Annexin V/PI dot plot and histograms, only cells gated in the FSC/SCC plot are shown. Cells with Annexin V+/PI- are the early apoptotic cells, and cells with Annexin V+/PI+ are the late apoptotic cells. (B) The flowcytometric plots of a 24-hr culture of cells labeled with ⁹⁹ᵐTc-HMPAO. Both cells with Annexin V+/PI- (early apoptotic cells) and cells with Annexin V+/PI+ (late apoptotic cells) are present in higher number as compared to normal controls.

phils, CC chemokines act on monocytes, but not neutrophils, and have additional activities toward basophil and eosinophil granulocytes as well as T-lymphocytes (*19*). The CC chemokines, monocyte chemotactic proteins MCP-1, MCP-2 and MCP-3 are major attractants for human CD4+ and CD8+ T lymphocytes, showing superior effectiveness when compared to other CC chemokines, such as macrophage inflammatory proteins MIP-1 alpha and MIP-1 beta or RANTES (regulated on activation, normal T cell expressed and secreted) (*20,21*). The monocyte chemotactic proteins probably play a major role in the recruitment of activated T-lymphocytes.

Hence, we used MCP-3 to evaluate chemotaxis of ⁹⁹ᵐTc-HMPAO-radiolabeled T-lympocytes, constituting approximately 60%–70% of the normal peripheral blood lymphocytes. Using a microwell Boyden chamber assay, we found chemotaxis of ⁹⁹ᵐTc-HMPAO-labeled T-lymphocytes to be reduced by approximately 31% as compared to both nonlabeled and HMPAO-labeled controls, both the latter showing no difference in migration index (Table 1). These results were assessed 4 hr after labeling with ⁹⁹ᵐTc-HMPAO corresponding to the normal time interval at which image acquisition is started.

The data presented suggest that, after labeling with ⁹⁹ᵐTc-HMPAO, a large fraction of labeled lymphocytes will still be able to respond to chemotaxis, supporting the clinical findings by Schauwecker et al. (*1*). The absence of a difference in migration index between nonlabeled and HMPAO-labeled cells suggests HMPAO does not influence lymphocytic chemotaxis. The reduction by 31% of chemotaxis in ⁹⁹ᵐTc-HMPAO-labeled T-lymphocytes as compared to both nonlabeled and HMPAO-labeled T-lymphocytes, however, points towards ionizing radiation damage induced by ⁹⁹ᵐTc as the main cause for this reduction.

The 24-hr radiation absorbed dose to lymphocytes labeled with 30 ± 23 μCi ⁹⁹ᵐTc/10⁶ lymphocytes is 11 ± 7 Gy. Interestingly, x-rays and gamma rays, when given in small to moderate doses, induce apoptosis without producing necrosis. This has been described in cells in the stem-cell region of hierarchically-arranged rapidly proliferating populations such as gut crypts (*22*), differentiating spermatogonia (*23*), rapidly

proliferating cells in the fetus (*24*) and lymphocytes (*25,26*). In addition, cells undergoing apoptosis are characterized by the formation of a highly cross-linked, rigid framework, probably due to an increase of tissue-type transglutaminase, which aids in the maintenance of cell and apoptotic bodies integrity and that may hypothetically limit chemotaxis (*6*).

In view of these findings, it may be expected that, after labeling with ⁹⁹ᵐTc-HMPAO, a certain fraction of lymphocytes will undergo apoptosis and that this fraction will correspond to the fraction of cells showing impaired chemotaxis. We looked at apoptosis of ⁹⁹ᵐTc-HMPAO-labeled lymphocytes, using flow cytometry light-scatter measurements and fluorescein isothiocyanate (FITC)-labeled Annexin V fluorescence (green fluorescence) combined with dye exclusion of propidium iodide (negative for red fluorescence), under the same environmental conditions as those of the chemotaxis assay. Whereas the mean percentages apoptotic lymphocytes in the nonlabeled, 18.5%, and HMPAO-labeled fractions, 16.6%, were more or less comparable (p = 0.1), the mean percentage apototic cells in the ⁹⁹ᵐTc-HMPAO-labeled fractions was 51.8%, yielding a difference of 33.3% between ⁹⁹ᵐTc-HMPAO-labeled and unlabeled cells. Since this 33.3% is quite close to the 31% observed in chemotaxis decrease, it seems plausible that the decreased chemotaxis is the result of the apoptotic process. The 31% decrease in chemotaxis at 4 hr (a time point at which the extent of apoptosis of irradiated lymphocytes is insufficiently depictable with FCM) as compared to the 33.3% increase of apoptotic cells at 24 hr (the optimal time point for apoptosis analysis with FCM) suggests chemotactic impairment in lymphocytes undergoing apoptosis precedes cell membrane inversion and increased permeability.

CONCLUSION

Using the Boyden microchamber assay, chemotaxis of ⁹⁹ᵐTc-HMPAO-labeled lymphocytes was found to be reduced by approximately 30%. Furthermore, the percentage apoptotic lymphocytes induced by irradiation after labeling with ⁹⁹ᵐTc-HMPAO concurs well with the percentage of chemotaxis impaired cells.

REFERENCES

1. Schauwecker DS, Burt RW, Park HM, et al. Comparison of purified indium-111 granulocytes and indium-111 mixed leucocytes for imaging of infections. *J Nucl Med* 1988;29:23–25.
2. Mortelmans L, Malbrain S, Stuyck J, et al. In vitro and in vivo evaluation of granulocyte labeling with 99mTc-HMPAO. *J Nucl Med* 1989;30:2022–2028.
3. Peters AM, Roddie ME, Danpure HJ. Technetium-99m-HMPAO-labeled leucocytes: comparison with 111In-troponolate-labeled granulocytes. *Nucl Med Commun* 1988;9:449–463.
4. Costa DC, Lui D, Ell P. White cells radiolabeled with 111In and 99mTc: a study of relative sensitivity and in vivo viability. *Nucl Med Commun* 1988;9:725–731.
5. Fesus L, Thomazy V. Searching for the function of tissue transglutaminase, its possible involvement in the biochemical pathway of programmed cell death. *Adv Exp Med Biol* 1988;231:119–134.
6. Fesus L, Davies PJA, Piacentini M. Apoptosis: molecular mechanisms in programmed cell death. *Eur J Cell Biol* 1991;56:170–177.
7. Kroemer G, Petit P, Zamzami N, Vayssi'8fre JL, Mignotte B. The biochemistry of programmed cell death. *FASEB J* 1995;9:1277–1287.
8. Kerr JFR, Winterford CM, Harmon BV. Apoptosis: its significance in cancer and cancertherapy. *Cancer* 1994;73:2013–2026.
9. Milner AE, Wang H, Gregory CD. Analysis of apoptosis by flow cytometry. In: Dekker M, ed. *Flow cytometry applications in cell culture.* 1996:193–209.
10. Thierens HMA, Vral AM, Van Haelst JP, Van de Wiele C, Schelstraete KHG, de Ridder LIF. Lymphocyte labeling with technetium-99m-HMPAO: a radiotoxicity study using the micronucleus assay. *J Nucl Med* 1992;33:1167–1174.
11. Proost P, Van Leuven P, Wuyts A, Ebberinck R, Opdenakker G, Van Damme J. Chemical synthesis, purification and folding of the human monocyte chemotactic proteins MCP-2 and MCP-3 into biologically active chemokines. *Cytokine* 1995;7:97–104.
12. Falk W, Goodwin RH Jr, Leonard EJ. A 48-well micro chemotaxis assembly for rapid and accurate measurement of leucocyte migration. *J Immunol Methods* 1980;33:239–247.
13. Dive C, Gregory CD, Phipps DJ, Evans DL, Milner AE, Wyllie AH. Analysis and discrimination of necrosis and apoptosis by multiparameter flow cytometry. *Biochem Biophys Acta* 1992;1133:275–279.
14. Martin SJ, Reutelingsperger CP, McGahon AJ, et al. Early redistribution of plasma membrane phosphatidylserine is a general feature of apoptosis regardless of the initiating stimulus:inhibition by overexpression of Bcl-2 and Abl. *J Exp Med* 1995;182:1545–1556.
15. Vermes I, Haanen C, Steffens-Naken H, Reutelingsperger CP. A novel assay for apoptosis. Flow cytometric detection of phosphatidylserine expression on early apoptotic cells using fluorescein-labeled Annexin V. *J Immunol Meth* 1995;184:39–51.
16. Deckers CLP, Lyons AB, Samuel K, Sanderson A, Maddy AH. Alternative pathways of apoptosis induced by methylprednisolone and valinomycin analysed by flow cytometry. *Exp Cell Res* 1993;208:362–365.
17. Oppenheim JJ, Zachariae COC, Mukaida N, Matsushima K. Properties of the novel proinflammatory supergene "intercrine" cytokine family. *Annu Rev Immunol* 1991;6:617–621.
18. Van Damme J. Interleukin-8 and related chemotactic cytokines. In: Thomson A, ed. *The cytokine handbook.* New York, NY: Academic Press Limited;1994:185–208.
19. Baggiolini M, Loetscher P, Moser B. Interleukin-8 and the chemokine family. *Int J Immunopharmacol* 1995;17:103–108.
20. Taub DD, Proost P, Murphy WJ, Anver M, Longo DL, Van Damme J, Oppenheim JJ. Monocyte chemotactic protein-1 (MCP-1), -2 and -3 are chemotactic for human T lymphocytes. *J Clin Invest* 1995;95:1370–1376.
21. Loetscher P, Seitz M, Clark-Lewis I, Baggiolini M, Moser B. Monocyte chemotactic proteins MCP-1, MCP-2 and MCP-3 are major attractants for human CD4+ and CD8+ T lymphocytes. *FASEB-J* 1994;8:1055–1060.
22. Potten CS. Extreme sensitivity of some intestinal crypt cells to x and gamma-irradiation. *Nature* 1977;269:518–521.
23. Allan DJ, Harmon BV, Kerr JFR. Cell death in spermatogenesis. In: Potten CS, ed. *Perspectives on mammalian cell death.* Oxford, England: Oxford University Press; 1987:229–258.
24. Gobé GC, Axelsen RA, Harmon BV, Allan DK. Cell death by apoptosis following x-irradiation of the fetal and neonatal rat kidney. *Int J Radiat Biol* 1988;54:567–576.
25. Sellins KS, Cohen JJ. Gene induction by gamma-irradiation leads to DNA fragmentation in lymphocytes. *J Immunol* 1987;139:199–206.
26. Yamad T, Ohyama H. Radiation-induced interphase death of rat thymocytes is internally programmed (apoptosis). *Int J Radiat Biol* 1988;53:65–75.

Sustained Right Ventricular Dyskinesis Complicated by Right Ventricular Infarction

Tomoaki Nakata, Akiyoshi Hashimoto, Atsushi Kuno, Kazufumi Tsuchihashi, Shuji Yonekura and Kazuaki Shimamoto

Second Department of Internal Medicine, Sapporo Medical University School of Medicine, Sapporo, Japan

We encountered a 66-yr-old man with acute left inferior and right ventricular infarction. Tomographic radionuclide ventriculography and Fourier analysis clearly demonstrated reduced wall motion in the inferior walls of both ventricles and markedly delayed phase angles in the inferior right ventricular segment, indicating dyskinesis, which was confirmed by two-dimensional echocardiography and contrast right ventriculography. Four years later, right ventricular dyskinesis was still present and corresponded to a right ventricular perfusion defect on 99mTc-labeled tetrofosmin tomogram. Right ventricular imaging with tomographic radionuclide ventriculography with Fourier analysis and 99mTc-labeled myocardial tomography demonstrates that, even after improved global function and hemodynamics, right ventricular dyskinesis related to right ventricular perfusion defect can be sustained for several years. Thus, these imaging techniques may contribute to diagnosing right ventricular infarction and investigating the pathophysiology.

Key Words: right ventricular infarction; radionuclide ventriculography; tetrofosmin scintigraphy; dyskinesis

J Nucl Med 1997; 38:1421–1423

Right ventricular (RV) infarction is an important complication of acute left ventricular inferior infarction, sometimes leading to hemodynamic deterioration and poor patient prognosis (1,2). Impairment of RV performance and hemodynamics due to RV infarction can improve spontaneously over time, typically within several days to a few weeks; sustained RV failure or wall motion abnormality is quite rare later (3). Poor clinical outcomes in RV infarct patients are due to generally hemodynamic deterioration, RV failure and arrhythmias at an acute phase, probably related to RV infarct size. Therefore, it is very important clinically to evaluate the presence and extent of RV infarction. However, unless hemodynamic or electrocardiographic alterations are manifested, RV infarction is often not diagnosed, probably because of difficulties in identifying regionally impaired RV perfusion and wall motion, which can be prolonged even after the recovery of global RV function (4,5). Technetium-99m-pyrophosphate scintigraphy is useful for delineating infarcted myocardium per se, but the availability is limited to several days following infarction. Two-dimensional echocardiography, which has proved to be of value for bedside monitoring of regional wall motion and predicting an increased RV pressure due to pump failure has technical limitations in some cases, and other conventional imaging modalities seem less useful. Recent advances in scintigraphic tomography may help to detect RV infarction-related dysfunction and perfusion abnormalities more precisely (6–8); that is, improvement of spatial and temporal resolutions for cardiac imaging can be achieved by 99mTc-labeled perfusion agents with an ideal